

# Active plasmonic devices based on $\epsilon$ -near-zero nonlinear metamaterials

A. Ciattoni<sup>1</sup>, C. Rizza<sup>2</sup>, E. Palange<sup>2</sup>

<sup>1</sup> Consiglio Nazionale delle Ricerche, CNR-SPIN  
67100 Coppito, L'Aquila, Italy

<sup>2</sup> Dipartimento di Ingegneria Elettrica e dell'Informazione, Università dell'Aquila  
67100 Monteluco di Roio, L'Aquila, Italy

## Abstract

We theoretically propose and numerically investigate an active plasmonic device made up of a nonlinear  $\epsilon$ -near-zero metamaterial slab of thickness smaller than 100 nanometers lying on a linear  $\epsilon$ -near-zero metamaterial substrate. In free-space coupling configuration and total reflection condition, we predict that the system can be regarded as a memory unit whose binary state is accessible by measuring either the phase difference between incident and reflected waves or the power carried by the nonlinear plasmon wave along the slab-substrate interface, both quantities displaying multivaluedness and hysteresis.

## 1. Introduction

Active plasmonics is mainly concerned with the manipulation of the plasmonic flow, on the photonic board, along the path between the source and the detector by means of a suitable external control of the dielectric refractive index near the metal surface [1]. Various methodologies have been proposed, encompassing electro-optic and nonlinear optical steering but they are fundamentally hindered by the involved very short propagation distances and, most importantly, by the weakness of the produced refractive index change. In order to achieve efficient plasmon steering we here propose to use  $\epsilon$ -near-zero nonlinear metamaterials since the small value of the permittivity allows the nonlinearity, no more playing the role of a weak perturbation, to deeply affect the light behavior [2].

## 2. Plasmonic Multistability and Hysteresis

The plasmonic device is made up of a slab of thickness  $L = 84 \text{ nm}$  lying on a substrate as reported in Figure 1a. Here we consider monochromatic electromagnetic radiation whose free-space wavelength is

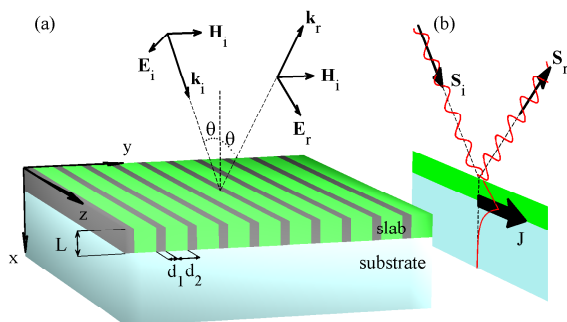


Figure 1: (a) Geometry of the plasmonic device (slab and substrate) and of the free-space incident (i) and reflected (r) plane waves (whose Poynting vectors are  $S_i$  and  $S_r$ ). (b) Sketch of the electromagnetic device configuration.  $J$  represents the overall power carried along the interface by the nonlinear surface mode.

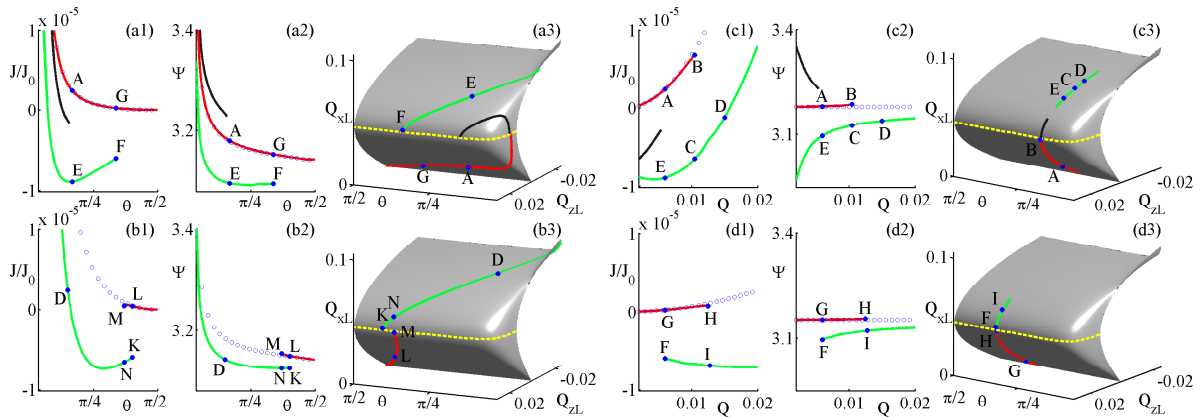


Figure 2: Plots of the normalized power per unit length  $J/J_0$  (here  $J_0 = \sqrt{\epsilon_0/\mu_0}/(2k_0\chi^{(3)})$ ) and phase difference  $\Psi$  along four possible ways of varying the excitation parameters. (a)  $Q = 0.006$  (fixed) and  $\theta_{cr} < \theta < \pi/2$  (variable); (b)  $Q = 0.015$  (fixed) and  $\theta_{cr} < \theta < \pi/2$  (variable); (c)  $0 < Q < 0.02$  (variable) and  $\theta = \pi/6$  (fixed); (d)  $0 < Q < 0.02$  (variable) and  $\theta = \pi/3$  (fixed). In each panel, the curves plotted by empty circles represent the linear counterparts of  $J$  or  $\Psi$ . The surface of allowed  $Q_{xL}$  is plotted in panels a3, b3, c3 and d3.

$\lambda = 810 \text{ nm}$ . The slab is a nonlinear Kerr metamaterial with permittivity  $\epsilon_{sl} = -0.01$  and nonlinear susceptibility  $\chi^{(3)} > 0$  whereas the substrate is a linear metamaterial with the permittivity  $\epsilon_{su} = 0.01$ . A way to synthesize these artificial media is to repeat along the  $y$ -axis nonlinear metal and active-dielectric layers with period  $d_1 + d_2$  much smaller than  $\lambda$  so that radiation experiences a uniform electromagnetic response obtained by averaging both the constituents linear permittivities and nonlinear Kerr susceptibilities [3]. As reported in Figure 1a, a  $p$ -polarized incident plane wave (i) is made to impinge onto the slab-vacuum interface (the plane  $x = 0$ ) with incidence angle  $\theta > \theta_{cr} = \arcsin \sqrt{\epsilon_{su}} \simeq 5.7^\circ$  so that total reflection occurs,  $|\mathbf{E}_r| = |\mathbf{E}_i| = Q/\sqrt{\chi^{(3)}}$ , the scattering solely producing the phase difference  $\Psi$  (given by  $e^{i\Psi} = \frac{\mathbf{E}_r \cdot \hat{\mathbf{e}}_x}{\mathbf{E}_i \cdot \hat{\mathbf{e}}_x}$ ) between the reflected and incident waves. As schematically sketched in Figure 1b, total reflection produces a nonlinear plasmon mode (which is a transverse magnetic (TM) field) localized at the interface  $x = L$  with energy flow purely along the  $z$ -direction (since the Poynting vector is  $\mathbf{S} = \frac{1}{2}\text{Re}(\mathbf{E} \times \mathbf{H}^*) = S_z(x)\hat{\mathbf{e}}_z$ ) and total power per unit length  $J = \int_0^\infty dx S_z(x)$ . We have numerically evaluated various nonlinear plasmon modes for a number of excitation states ( $\theta$ ,  $Q$ ) and obtained the corresponding  $J$  and  $\Psi$  which are reported in Figure 2 along four possible ways (denoted with a, b, c and d) of varying the parameters ( $\theta$ ,  $Q$ ) (as detailed in the figure caption). Note that, in each situation, the system displays multistability since both  $J$  and  $\Psi$  are multi-valued function of  $\theta$  and  $Q$ . It is evident that the values of  $J$  and  $\Psi$  lie on at most three different branches and, most importantly, that the branches presents points at which they abruptly stop. System multi-stability is a consequence of the field matching at interface  $x = L$ , i.e.  $[\epsilon_{sl} + \frac{1}{2}(3Q_{xL}^2 + Q_{zL}^2)]Q_{xL} + \epsilon_{su}\sqrt{\frac{\sin^2\theta}{\sin^2\theta - \epsilon_{su}}}Q_{zL} = 0$  where  $Q_{xL}$  and  $Q_{zL}$  are  $x$  and  $z$  dimensionless electric field components at the interface  $x = L$  on the slab side. Since  $|\epsilon_{sl}| \ll 1$ , the nonlinear term in the bracket cannot be neglected and therefore, for  $\theta$  and  $Q_{zL}$  assigned, this equation provides more than one allowed values of  $Q_{xL}$  as is particularly evident from panels a3, b3, c3 and d3 of Figure 2 where the ensuing folded surface  $Q_{xL}$  is plotted. System hysteresis easily follows from the discussed phenomenology. Suppose, for example, that the incident plane wave is such that  $\theta = \pi/3$  and  $Q = 0.001$  so that, from panels d1, d2 and d3 of Figure 2, it is evident that a state of the upper branch is excited since for  $Q < 0.004$  the lower branch has no corresponding allowed states. By increasing the input intensity (and hence  $Q$ ) the state  $G$  is reached and surpassed toward the state  $H$ . Once  $H$  is reached, if the input intensity is further increased the system has to undergo a sudden jump to the state  $I$  belonging to the lower branch since the upper branch stops at  $H$ . From the state  $I$

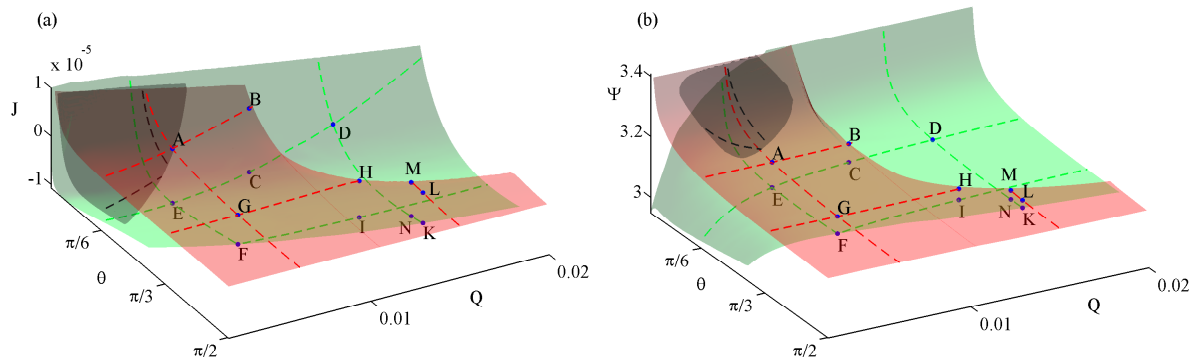


Figure 3: Global multi-valued surfaces of the normalized power per unit length  $J/J_0$  (a) and of the phase difference  $\Psi$  (b). Dashed lines represent the branches of  $J$  and  $\Psi$  considered in Figure 2.

the input intensity can now be decreased toward the state  $F$  and therefore along such a backward path the attained values of  $J$  and  $\Psi$  are different from the forward path, i.e. hysteresis occurs. Evidently, by decreasing the input intensity from the state  $F$  the system undergoes another jump to reach the state  $G$ , thus coming back to the upper branch and closing the hysteresis loop.

The number of possible hysteresis loops is infinite since  $\theta$  and  $Q$  can independently be varied. In Figure 3 we plot the values of  $J$  and  $\Psi$  for all the possible  $\theta$  and  $Q$  in the ranges  $\theta_{cr} < \theta < \pi/2$  and  $0 < Q < 0.02$ . The surfaces representing  $J$  and  $\Psi$  exhibit more than one sheet, each one admitting breaking lines, and the position of the just discussed hysteresis loop G-H-I-F is particularly evident. If we choose to operate uniquely with the two considered sheets, it is evident that the system is suitable to record a binary information which can easily be read since a single measure of  $\Psi$  (or  $J$ ) allows to know whether the system state belongs to the upper or the lower sheet. Moreover, the state of the memory unit can be simply changed by driving the system through a breaking line thus forcing a switch of its operating sheet. Note also that the system memory functionality can even be suitably tailored to satisfy external requirements (i.e. specific optical intensities or angles imposed by a possible nearby circuit environment) since, for each plasmonic state, a hysteresis loop can be found which starts and ends at the considered state. Suppose, as an example, that an hysteresis loop containing the state  $A$  of Figures 2 and 3 is required. Once the state  $A$  is excited, one can increase the field amplitude  $Q$  to reach the state  $B$  (which is a breaking point of its sheet) and to force the system to jump to the state  $C$ . From panel c1 and c2 of Figure 2 or from Figure 3 it is apparent that by solely varying the field amplitude the system can never be brought back to the state  $A$ . However, one can drive the system to reach the state  $E$ , fix the field amplitude  $Q$  and increase the angle  $\theta$  to reach the state  $F$  (see panel a1 and a2 of Figure 2 or Figure 3) which is a breaking point of the lower sheet. Therefore a jump can be induced to make the system reach the state  $G$  belonging to the upper sheet and, after reducing the angle, to come back to the initial state  $A$  thus closing the hysteresis loop. Note that the intensity of the incident plane wave is  $I = (1/2)\sqrt{\epsilon_0/\mu_0}Q^2/\chi^{(3)}$  which, for the amplitude range  $Q < 0.02$  (where multistability occurs for  $\epsilon_{sl} = -0.01$ ) and for  $\chi^{(3)} = 9 \cdot 10^{-17} \text{m}^2/\text{V}^2$ , yields  $I < 1.17 \text{ MW}/\text{cm}^2$ , which are intensities smaller than those normally required for observing the standard optical bistability.

## References

- [1] K. F. MacDonald and N. I. Zheludev, *Laser Phot. Rev.* **4**, 562 (2010).
- [2] A. Ciattoni, C. Rizza and E. Palange, "All-optical active plasmonic devices with memory and power switching functionalities based on  $\epsilon$ -near-zero nonlinear metamaterials", accepted for publication on *Physical Review A*.
- [3] A. Ciattoni, C. Rizza and E. Palange, *Phys. Rev. A* **81**, 043839 (2010).